LETTERS

Chaotic capture of Jupiter's Trojan asteroids in the early Solar System

A. Morbidelli[1], H. F. Levison[1,2], K. Tsiganis[1] & R. Gomes[1,3]

Jupiter's Trojans are asteroids that follow essentially the same orbit as Jupiter, but lead or trail the planet by an angular distance of ~60 degrees (co-orbital motion). They are hypothesized to be planetesimals that formed near Jupiter and were captured onto their current orbits while Jupiter was growing[1,2], possibly with the help of gas drag[3–6] and/or collisions[7]. This idea, however, cannot explain some basic properties of the Trojan population, in particular its broad orbital inclination distribution, which ranges up to ~40 degrees (ref. 8). Here we show that the Trojans could have formed in more distant regions and been subsequently captured into co-orbital motion with Jupiter during the time when the giant planets migrated by removing neighbouring planetesimals[9–12]. The capture was possible during a short period of time, just after Jupiter and Saturn crossed their mutual 1:2 resonance, when the dynamics of the Trojan region were completely chaotic. Our simulations of this process satisfactorily reproduce the orbital distribution of the Trojans and their total mass.

Recent numerical experiments[13,14] have shown that the orbits of the giant planets are best reproduced if Saturn and Jupiter crossed their mutual 1:2 mean motion resonance (MMR) during their migration. This occurs when the ratio of their orbital periods, P_S/P_J, equals 2. The current ratio of P_S/P_J is slightly less than 2.5. However, there is a serious argument in the literature against the idea that Jupiter and Saturn crossed the 1:2 MMR. If the crossing had happened, any pre-existing jovian Trojans would have become violently unstable, and Jupiter's co-orbital region would have emptied[15,16]. Indeed, we performed a simulation similar to that in ref. 15, but with 1.3 million particles in the Trojan region—none survived the 1:2 MMR crossing.

However, the dynamical evolution of a gravitating system of objects is time reversible. Thus, if the local objects can escape the Trojan region when the latter becomes unstable, other bodies can enter the same region and be temporarily trapped. Consequently, a transient Trojan population can be created if there is an external source of objects. In this case, the source is constituted by the very bodies that are forcing the planets to migrate[9–12], and is of considerable magnitude given how much the planets must move. When Jupiter and Saturn get far enough from the 1:2 MMR that the co-orbital region becomes stable, the population that happens to be there at that time remains trapped. It becomes the population of permanent jovian Trojans still observable today.

To investigate the above idea, we first performed a numerical simulation that involved integrating the orbits of a series of massless planetesimals initially on Saturn-crossing orbits under the gravitational influence of the Sun, Jupiter and Saturn. In this simulation, the planets were on non-migrating orbits close to the 1:2 MMR, so that the Trojan region was fully unstable. We found that ~1% of the planetesimals initially on Saturn-crossing orbits spent more than 100 yr as jovian Trojans, which we define as objects having orbital periods relative to Jupiter's of between 0.97 and 1.03, absolute values of angular distance from the planet of between 40° and 90°, and eccentricities of less than 0.15. These values were derived from the current orbital distribution of the Trojans. The particles temporarily trapped in the Trojan region covered the whole region of co-orbital motion. More importantly, their orbital inclination covered all values up to ~40°, as a result of previous close encounters with the planets. Therefore, our idea became appealing because it could potentially explain the puzzling broad inclination distribution of the jovian Trojans. Motivated by this possibility, we proceeded with a far more comprehensive, and time consuming, set of simulations of this idea.

The first step in this expanded study was to determine exactly when the Trojans become unstable during the resonant crossing. For this purpose, we started by adopting the migration rates from one of the simulations reported in ref. 13. In particular, we chose a simulation where the planets migrated relatively slowly. From that simulation we measured the ratio P_S/P_J at 40 timesteps (Fig. 1a). Then, we performed 40 orbital integrations of massless test particles under the influence of the Sun, Jupiter and Saturn. The planets were placed on non-migrating orbits, with the same values of P_S/P_J as measured in Fig. 1a. The initial distribution of test particles was chosen to mimic the current distribution of Trojans relative to Jupiter. Each simulation covered 2×10^5 yr, and the fraction of the initial test particle population that remained in the Trojan region is reported in Fig. 1b, where each simulation is represented by a single point. We note two planetary configurations that are critical for the survivability of the Trojans. One occurs when $P_S/P_J \approx 2.05$ (time $t = 4.5 \times 10^5$ yr in the reference simulation), at which point all resident Trojans escape. This indicates that the entire co-orbital region is particularly unstable at this time. This instability is due to a secondary 3:1 resonance[17] between $(1/P_J–2/P_S)$ and the oscillation frequency of the Trojans around the Lagrange point. The other critical configuration occurs when $P_S/P_J \approx 2.08$ ($t = 10^6$ yr), which corresponds to a secondary 2:1 resonance between the same two frequencies, and depletes 70% of the Trojans.

In our scheme, the capture of jovian Trojans had to have occurred during these two critical planetary configurations. Thus, we designed a pair of simulations intended to study the capture process. In the first of these simulations (referred to as the slow simulation hereafter), we adopted the same migration rate as in the last paragraph. Jupiter and Saturn were forced to migrate by including a suitably chosen drag term in the planets' equations of motion, as prescribed in ref. 10, so that they reproduced the evolution of P_S/P_J shown in Fig. 1a. From 3.5×10^5 yr (just before the first critical configuration is reached) to 1.2×10^6 yr (just after the second critical configuration has passed), we supplied a steady flux of 5,466,000 planetesimals through the Jupiter–Saturn system (see Methods). This simulation

[1]Observatoire de la Côte d'Azur, BP 4229, 06304 Nice Cedex 4, France. [2]Department of Space Studies, Southwest Research Institute, 1050 Walnut Street, Suite 400, Boulder, Colorado 80302, USA. [3]GEA/OV/UFRJ and ON/MCT, Ladeira do Pedro Antonio, 43-Centro 20.080-090, Rio de Janeiro, RJ, Brazil.

covered 10 Myr, at which point the orbits of the planets were sufficiently close to their observed ones. The second simulation was identical to the first, but with a migration rate that was three times larger and an integration time three times shorter. We will refer hereafter to this as the fast simulation. Comparably fast migration rates have been observed in many of the runs in ref. 13.

At the end of the slow simulation, 2.4×10^{-6} of the planetesimals were found to be on orbits trapped in the Trojan region. The capture efficiency rises to 1.8×10^{-5} in the fast simulation. Of these trapped Trojans, ~50% (the same ratio in both simulations) have libration amplitudes (the semi-amplitude of the oscillation of the angular distance from Jupiter) smaller than 30°, like 87% of the known Trojans. The vast majority of the captured Trojans with larger amplitudes of libration would not survive up to current times, because their dynamics are unstable on long timescales[18]. Thus, we restrict the analysis of our fictitious Trojans to those objects with libration amplitudes less than 30°.

In terms of total mass (see Methods for a description of the mass estimates), our trapped Trojan population is quite consistent with the real population, when scaled to the mass required to move the planets the required distance. Our slow simulation predicts a total Trojan mass of $\sim 4 \times 10^{-6} M_E$ (where M_E is the Earth's mass), where the fast simulation predicts a mass of $\sim 3 \times 10^{-5} M_E$. Using the most up-to-date observations, we estimate the mass of the Trojan population with $D < 30°$ to be $1.1 \times 10^{-5} M_E$. So, the actual mass of the Trojans appears to be in the range predicted by our two simulations.

The reason why the mass trapped in the Trojan region increases so sharply with the planetary migration rate is twofold. First, a faster migration rate corresponds to a proportionally higher mass flux. Thus, the transient population that resides in the co-orbital region when this region is chaotic is proportionally enhanced. This explains a factor of about three between the results of the two simulations. Second, faster migration results in a sharper transition from instability to stability in the co-orbital region, which increases the fraction of the transient population that becomes permanently trapped. This probably explains the remaining factor of ~7/3 between the results of the two simulations.

Figure 2 shows the distribution of the captured Trojans in the space of the three fundamental orbital parameters that characterize co-orbital dynamics: the proper eccentricity *e*, inclination *i* and libration amplitude *D*. ('Proper' refers to parameters that are suitably averaged over short periods of time and is usually introduced to characterize oscillating orbits[19].) Their computation is explained in Methods. Because the distribution of the captured objects is similar in both simulations, we have included both data sets in Fig. 2 in order to improve statistics. The distribution of the known Trojans is also plotted, for visual comparison. There is an excellent qualitative agreement between the observed and simulated distributions. The captured Trojans cover the same range of values of the orbital parameters as the observed ones. There is no macroscopic region of orbital parameter space that is both occupied by the real Trojans and is left empty by the simulated ones. In particular, simulated Trojans are found even on orbits with $D < 5°$. These orbits are the hardest to populate, in any capture model[8]. We stress that the inclinations of the trapped Trojans range from 0° to 40°, like those of the observed population.

We note that our results may provide an explanation for why jovian Trojans look so similar to cometary nuclei and to some (the bluest) Centaurs and Kuiper belt objects at visible wavelengths[20,21]. In fact, it has been argued that both the Kuiper belt[22,23] and the scattered disk[24]—which is the current source of Centaurs and Jupiter-family comets, and probably also the progenitor of the Oort cloud—

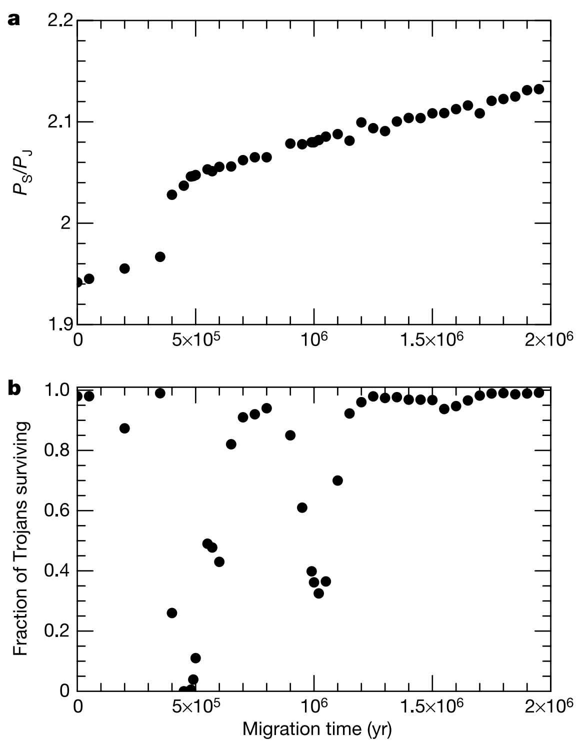

Figure 1 | The stability of Trojans during planetary migration. a, The temporal evolution of the ratio of orbital periods of Saturn and Jupiter (P_S and P_J, respectively) from the migration simulation that we chose from ref. 13. The magnitude of the jump in P_S/P_J when the planets cross $P_S/P_J = 2$ reflects the width of the 1:2 MMR. The planets are not captured into resonance but jump over it. **b**, The fraction of the Trojan population that survives for 2×10^5 yr in the co-orbital region, as a function of P_S/P_J (and hence of migration time).

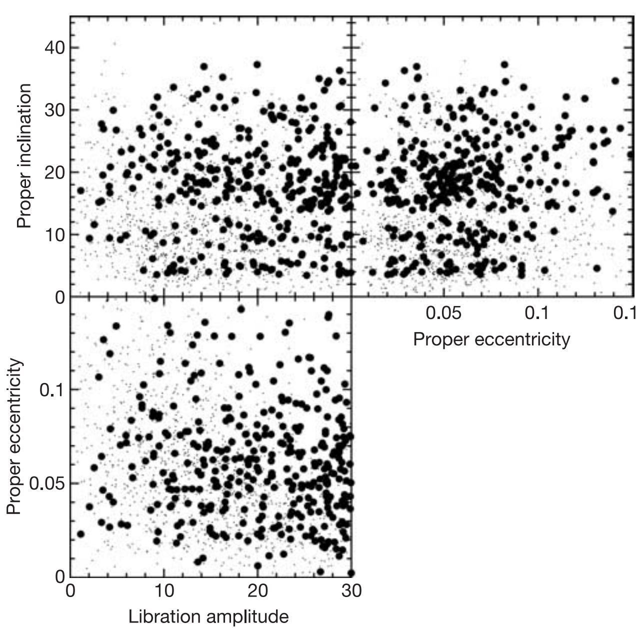

Figure 2 | Comparison of the orbital distribution of Trojans between model and observations. The simulation results are shown as filled circles and the observations as dots in the space of the three orbital parameters for co-orbital motion. The distribution of the simulated Trojans is somewhat skewed towards large libration amplitudes, relative to the observed population. However, this is not a serious problem because a fraction of the planetesimals with the largest amplitudes would leave the Trojan region during the subsequent 4 Gyr of evolution[18], leading to a better match. The similarity between the two inclination distributions is strong support for our model. Libration amplitude and proper inclination are measured in degrees.

originated in the planetesimal disk that drove planetary migration. Our model places the origin of jovian Trojans in the same parent population.

Our results may also prove an explanation for the fact that Trojans are apparently deficient in water and organics[25]. Before being captured in the Trojan region, planetesimals typically evolved through a large eccentricity phase that brought them relatively close to the Sun. Indeed, all the particles that spent more than 100 yr in the Trojan region in our first simulation reached a perihelion distance q of less than ~ 3 AU. Of them, 72% spent more than 10,000 yr on orbits with $q < 3$ AU, and 68% even reached $q < 2$ AU. Because it takes roughly 10,000 yr for an active Jupiter-family comet to become dormant[26], it is possible that the surfaces of the Trojans could have been devolatilized during their high eccentricity phase.

Our simulation shows that objects captured into Jupiter's co-orbital regions immediately after Jupiter and Saturn crossed the 1:2 MMR have an orbital distribution remarkably similar to that of the observed Trojans. In addition, it shows that the capture efficiency can explain the total number of objects observed. As our model is the only one available that can explain these features, we believe that the Trojans represent observational evidence for this resonance crossing, which has also been shown elsewhere[13] to produce the correct planetary orbits. Thus, this work, together with refs 13 and 14, provides a self-consistent view of the formation and primordial evolution of the Solar System.

METHODS

Simulation of Trojan capture. We start with our 'slow' simulation, where Jupiter and Saturn are forced to migrate as in Fig. 1a. The flux of planetesimals is modelled by setting test particles on Saturn crossing orbits with orbital periods larger than P_S and a distribution of eccentricities and inclinations that mimic that in our reference simulation from ref. 13 when the 1:2 MMR is crossed. Every time that a test particle is dynamically eliminated, it is reintroduced on its original trans-saturnian orbit rescaled to the current position of Saturn. In this way, the number of particles in the simulation at any time is constant (1,163,000) and their orbital distribution remains in steady state. In total, 5,466,000 particles are eliminated and reintroduced during the considered time-span. At $t = 1.2 \times 10^6$ yr, when the co-orbital region becomes stable again, 98 particles are found on Trojan-like orbits. These particles are each cloned 19 times. The integration is then continued with the planets migrating, for 10 Myr, until the planets come reasonably close to their current semimajor axes. A drag force is also added to the planets' equations of motion, in order to slowly damp their eccentricities to their current values. At the end of the simulation, 266 particles are in the Trojan region. The final trapping efficiency is 266/20/5,466,000 $\approx 2.4 \times 10^{-6}$.

In the 'fast' simulation, the migration rate of the planets is increased by a factor of three. A total of 2,773,000 particles are eliminated and reintroduced. 174 particles are found to be on Trojan-like orbits at the end of the second 'critical planetary configuration'. Of these particles, cloned 9 times each, 486 survive in the Trojan region at the end of planetary migration. The final trapping efficiency is 486/10/2,773,000 $\approx 1.8 \times 10^{-5}$.

The above simulations did not take into account Uranus and Neptune. These planets could affect the capture of Trojans in two ways. Immediately after the 1:2 MMR crossing they provided kicks to Saturn during close encounters. Thus, we modify the first stage of the above simulations by including stochastic kicks to Saturn every 150,000 years with a magnitude of 0.53 km s^{-1} (based on ref. 13). Then during the post-capture, 10 Myr migration, Uranus and Neptune could destabilize the Trojans by generating additional resonances. Thus, we perform again the second stage simulation, but including Uranus and Neptune. These planets are forced to migrate from 16.5 and 20 AU to their current positions, while their eccentricities are damped from 0.1. We find that the inclusion of the ice giants does not affect Trojan capture.

Estimates of Trojan mass. According to ref. 13, $\sim 3.4\,M_E$ of planetesimals are cycled through the system as the planets migrate through the unstable Trojan configurations. Of the trapped planetesimals, $\sim$50% are in the region $D < 30°$. The mass of captured Trojans is the product of $3.4\,M_E$, 0.5, and the capture efficiency of the corresponding simulation.

According to ref. 27, the current mass of the Trojans is $\sim$3–25 times larger than the value we find. However, ref. 27 probably overestimated the real value because it assumed: (1) an outdated density of 2 g cm^{-3}, whereas it is now believed to be $\rho = 1.3$ g cm^{-3} (refs 28, 29); (2) an outdated mean albedo $p_v = 0.04$, whereas later observations[20] showed that it is probably $p_v = 0.056$, and (3) an absolute magnitude (H) distribution that predicts 2.5 times more objects with $H < 11$ than observed.

Correcting for (1) and (2), while keeping the H-distribution shown in Fig. 9 of ref. 2 reduces the Trojan mass estimate to $2.5 \times 10^{-5}\,M_E$. Correcting for (3) requires a more involved procedure. Reference 27 constrains the slope of the H-distribution for $H > 10.5$, but their estimate of the total number is problematic because of the paucity of bright objects observed in their narrow field deep survey. To overcome this problem, we use the most recent catalogue of Trojan bodies (http://Hamilton.unipi.it/cgi-bin/astdys/astibo) which, according to SDSS findings (Gy. M. Svabo and Z. Ivezic, personal communication) is complete up to $H = 11.5$. Beyond this threshold we extrapolate the catalogue's distribution using the slope given in ref. 27. This reduces the total mass of the Trojans to $1.3 \times 10^{-5}\,M_E$, 87% of which is in the considered $D < 30°$ region.

Computation of Trojan proper elements. We integrate each Trojan orbit for 10^5 yr under the gravitational influence of only the Sun and Jupiter. No planetary migration is imposed. The numerical output is digitally filtered[30] in order to eliminate the short periodic oscillations of the orbital elements. The libration amplitude D is computed as $(\delta\lambda_{max} - \delta\lambda_{min})/2$, where $\delta\lambda$ is the difference between the mean longitude of the Trojan and of Jupiter, and the suffices min and max denote, respectively, its minimal and maximal value over a libration cycle. The proper eccentricity is computed as $(k_{max} - k_{min})/2$, where $k = e \sin \varpi$, ϖ is the Trojan's perihelion longitude and $k_{max/min}$ are computed over a secular oscillation of the Trojan's orbit. The proper inclination is computed in a similar way. This procedure is consistent with that used in ref. 19 for the real Trojans, which allows a direct comparison in Fig. 2.

Received 6 December 2004; accepted 11 March 2005.

1. Marzari, F. & Scholl, H. Capture of Trojans by a growing proto-Jupiter. *Icarus* **131,** 41–51 (1998).
2. Fleming, H. J. & Hamilton, D. P. On the origin of the Trojan asteroids: Effects of Jupiter's mass accretion and radial migration. *Icarus* **148,** 479–493 (2000).
3. Yoder, C. F. Notes on the origin of the Trojan asteroids. *Icarus* **40,** 341–344 (1979).
4. Peale, S. J. The effect of the nebula on the Trojan precursors. *Icarus* **106,** 308–322 (1993).
5. Kary, D. M. & Lissauer, J. J. Nebular gas drag and planetary accretion. II. Planet on an eccentric orbit. *Icarus* **117,** 1–24 (1995).
6. Kortenkamp, S. J. & Hamilton, D. P. Capture of Trojan asteroids in the early Solar Nebula. *Bull. Am. Astron. Soc.* **33,** 1086 (2001).
7. Shoemaker, E. M., Shoemaker, C. S. & Wolfe, R. F. in *Asteroids II* (eds Binzel, R. P., Gehrels, T. & Matthews, M. S.) 487–523 (Univ. Arizona Press, Tucson, 1989).
8. Marzari, F., Scholl, H., Murray, C. & Lagerkvist, C. in *Asteroids III* (eds Bottke, W. F., Cellino, A., Paolicchi, P. & Binzel, R. P.) 725–738 (Univ. Arizona Press, Tucson, 2002).
9. Fernandez, J. A. & Ip, W. H. Some dynamical aspects of the accretion of Uranus and Neptune—The exchange of orbital angular momentum with planetesimals. *Icarus* **58,** 109–120 (1984).
10. Malhotra, R. The origin of Pluto's peculiar orbit. *Nature* **365,** 819–821 (1993).
11. Hahn, J. M. & Malhotra, R. Orbital evolution of planets embedded in a planetesimal disk. *Astron. J.* **117,** 3041–3053 (1999).
12. Gomes, R. S., Morbidelli, A. & Levison, H. F. Planetary migration in a planetesimal disk: why did Neptune stop at 30 AU? *Icarus* **170,** 492–507 (2004).
13. Tsiganis, K., Gomes, R., Morbidelli, A. & Levison, H. F. Origin of the orbital architecture of the giant planets of the Solar System. *Nature* doi:10.1038/nature03539 (this issue).
14. Gomes, R., Tsiganis, K., Morbidelli, A. & Levison, H. F. Origin of the cataclysmic Late Heavy Bombardment period of the terrestrial planets. *Nature* doi:10.1038/nature03676 (this issue).
15. Gomes, R. S. Dynamical effects of planetary migration on primordial Trojan-type asteroids. *Astron. J.* **116,** 2590–2597 (1998).
16. Michtchenko, T. A., Beaugé, C. & Roig, F. Planetary migration and the effects of mean motion resonances on Jupiter's Trojan asteroids. *Astron. J.* **122,** 3485–3491 (2001).
17. Kortenkamp, S. J., Malhotra, R. & Michtchenko, T. Survival of Trojan-type companions of Neptune during primordial planet migration. *Icarus* **167,** 347–359 (2004).
18. Levison, H. F., Shoemaker, E. M. & Shoemaker, C. S. Dynamical evolution of Jupiter's Trojan asteroids. *Nature* **385,** 42–44 (1997).
19. Milani, A. The Trojan asteroid belt: Proper elements, stability, chaos and families. *Celest. Mech. Dyn. Astron.* **57,** 59–94 (1993).
20. Fernández, Y. R., Sheppard, S. S. & Jewitt, D. C. The albedo distribution of Jovian Trojan asteroids. *Astron. J.* **126,** 1563–1574 (2003).
21. Barucci, M. A., Cruikshank, D. P., Mottola, S. & Lazzarin, M. in *Asteroids III*

(eds Bottke, W. F., Cellino, A., Paolicchi, P. & Binzel, R. P.) 273–288 (Univ. Arizona Press, Tucson, 2002).
22. Gomes, R. S. The origin of the Kuiper Belt high-inclination population. *Icarus* **161,** 404–418 (2003).
23. Levison, H. F. & Morbidelli, A. The formation of the Kuiper belt by the outward transport of bodies during Neptune's migration. *Nature* **426,** 419–421 (2003).
24. Duncan, M. J. & Levison, H. F. A scattered comet disk and the origin of Jupiter family comets. *Science* **276,** 1670–1672 (1997).
25. Emery, J. P. & Brown, R. H. The surface composition of Trojan asteroids: constraints set by scattering theory. *Icarus* **170,** 131–152 (2004).
26. Levison, H. F. & Duncan, M. J. From the Kuiper Belt to Jupiter-family comets: The spatial distribution of ecliptic comets. *Icarus* **127,** 13–32 (1997).
27. Jewitt, D. C., Trujillo, C. A. & Luu, J. X. Population and size distribution of small Jovian Trojan asteroids. *Astron. J.* **120,** 1140–1147 (2000).
28. Merline, W. J. *et al.* in *Asteroids III* (eds Bottke, W. F., Cellino, A., Paolicchi, P. & Binzel, R. P.) 289–314 (Univ. Arizona Press, Tucson, 2002).
29. Britt, D. T., Yeomans, D., Housen, K. & Consolmagno, G. in *Asteroids III* (eds Bottke, W. F., Cellino, A., Paolicchi, P. & Binzel, R. P.) 485–500 (Univ. Arizona Press, Tucson, 2002).
30. Quinn, T. R., Tremaine, S. & Duncan, M. A three million year integration of the earth's orbit. *Astron. J.* **101,** 2287–2305 (1991).

Acknowledgements R.G. is grateful to the Conselho Nacional de Desenvolvimento Científico e Tecnológico for financial support of his sabbatical year in the OCA observatory in Nice. The work of K.T. was supported by an EC Marie Curie Individual Fellowship. A.M. and H.F.L. thank the CNRS and the NSF for funding the collaboration between the OCA and the SWRI groups. H.F.L. is grateful to NASA's Origins and PG&G programmes.

Author Information Reprints and permissions information is available at npg.nature.com/reprintsandpermissions. The authors declare no competing financial interests. Correspondence and requests for materials should be addressed to A.M. (morby@obs-nice.fr).